Statistical analysis

All data were analyzed using a commercial statistical software package (StatView, version 5.0J; SAS Institute, Cary, NC). Statistical analysis was performed to compare the L/N ratios among 3 groups (prior to SRT, at 3 months after SRT, and at 6 months after SRT) by using nonparametric Friedman's test. For all statistics, a probability value less than .05 was considered significant. All data are expressed asmeans ± SD.

Results

Follow-up studies were performed in all 42 tumors at 3 months after SRT-IMRT and in 24 tumors at 6 months after SRT-IMRT. Eighteen tumors of 8 patients were lost to follow-up 6 months after SRT-IMRT because those patientsdied from systemic disease within 6 months after SRT-IMRT.

In 23 of a total of 42 tumors, MRI with PET-based GTV was larger than MRI-based GTV. The average GTV defined by MRI alone was 8.01 ± 11.83 cm^3, and the average GTV defined by MRI with PET was 8.94 ± 12.29 cm^3. The average GTV increased by 10.4% when MRI with PET was used vs when MRI alone was used.

Results of the follow-up studies of quantitative analyses in all tumors are shown in Figure 2. L/N ratios were 1.95 ± 0.83, 1.18 ± 0.21, and 1.12 ± 0.25 in the pre-SRT-IMRT group, in the 3 month post-SRT-IMRT group, and in the 6 month post-SRT-IMRT group, respectively. Differences in the L/N ratios between the pre-SRT-IMRT group and the 3-month post-SRT-IMRT group was significant ($P<.0001$) and that between the pre-SRT-IMRT group and the 6-month post-SRT-IMRT group was also significant ($P<.0001$).

Results of analyses in each type classified by the volume change of Gd-DTPA enhancement are shown in Figure 3A, B, and C. The number of tumors in each type was 28, 7, and 7, respectively. In type A, the L/N ratios were 1.93 ± 0.98, 1.14 ± 0.19, and 1.05 ± 0.14 in the pre-SRT-IMRT, the 3-month post-SRT-IMRT group, and the 6-month post-SRT-IMRT group. In type B, the L/N ratios were 1.96 ± 0.28, 1.17 ± 0.26, and 1.11 ± 0.29 in the pre-SRT-IMRT group, the 3-month post-SRT-IMRT group, and the 6-month post-SRT-IMRT group. In type C, the L/N ratios were 2.04 ± 0.59, 1.31 ± 0.23, and 1.30 ± 0.35 in the pre-SRT-IMRT group, the 3-month post-SRT-IMRT group, and the 6-month post-SRT-IMRT group. In each of the 3 types, the differences in the L/N ratios between the pre-SRT-IMRT group and the 3-month post-SRT-IMRT group were significant ($P=.0001$ in type A; $P=.0003$ in type B; and $P=.0172$ in type C), and those between the pre-SRT-IMRT group and the 6-month post-SRT-IMRT group were also significant ($P=.0005$ in type A; $P=.0002$ in type B; and $P=.0294$ in type C).

Local recurrence was defined in two of a total of 42 tumors after SRT-IMRT. No recurrence was demonstrated in all tumors of type A. In one tumor of type B, the L/N ratio was decreased from 1.52-1.30 at 3 months after SRT-IMRT, but it was increased to

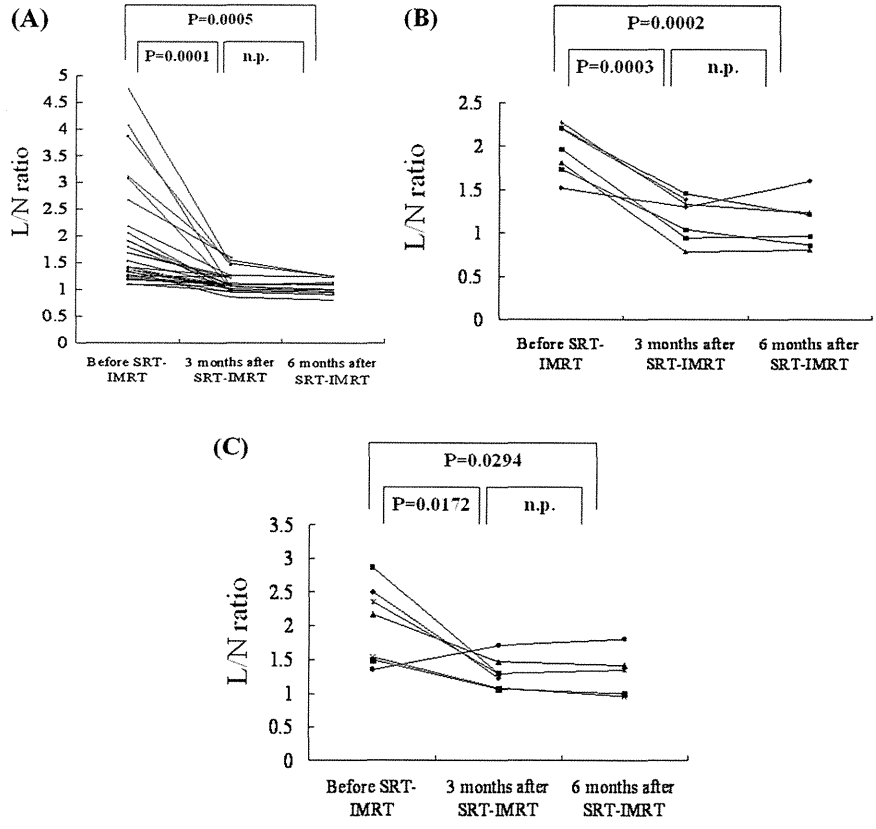

Fig. 3. The L/N ratio plotted at the PTV prior to SRT-IMRT, at 3 months after SRT-IMRT, and at 6 months after SRT-IMRT in each type classified by MRI examination. Complete response or partial response (A), no change (B), or progressive disease (C), all determined by the changes in the volume of contrast enhancement 3 months after SRT-IMRT. The number of tumors in each type was 28, 7, and 7, respectively. In each of the 3 types, differences in the L/N ratios between the pre-SRT-IMRT group and the 3-month post-SRT-IMRT group was significant ($P=.0001$ in type A; $P=.0003$ in type B; and $P=.0172$ in type C) and that between the pre-SRT-IMRT group and the 6-month post-SRT-IMRT group was also significant ($P=.0005$ in type A; $P=.0002$ in type B; and $P=.0294$ in type C).

1.60 in the next 3 months, and marginal tumor recurrence was defined at 9 months after SRT-IMRT. In one tumor of type C, the L/N ratio was increased from 1.34-1.71 at 3 months after SRT-IMRT, and marginal tumor recurrence was defined at 6 months after SRT-IMRT. In the other 6 tumors of type C, the L/N ratio was decreased after SRT-IMRT, and lesions showed spontaneous shrinkage or remained stable in size after a long-term follow-up, which were assumed to be radiation necrosis. Follow-up terms of these 6 tumors ranged from 19-43 months. A representative case of type C is shown in Figure 4. In the acute and subacute phases, there was no neurologic toxicity from SRT-IMRT in all cases.

Discussion

The use of PET, an imaging technique providing metabolic data, may play an important role in improving the radiosurgical treatment of malignant brain tumors (1-3, 8-10). In recent PET studies, analysis of the metabolic and histological characteristics of a stereotactic biopsy specimen provided evidence that regional high MET uptake correlated with the presence of viable tumor cells (11). Baumert et al (12) demonstrated the data correlated MRI findings with histology, in which an infiltrative growth beyond the border of the brain metastasis in 63% cases evaluated. Along the same line, the relationship between pathology and metabolism found in stereotactic biopsy and the increased knowledge about MET-PET in brain tumor strengthen the valuable link between MET uptake and histology. Matsuo et al (13) demonstrated that there was severe discrepancy between PET- and MRI-defined target volumes in their report of metastatic brain tumors, and those findings suggested that MET-PET might significantly improve the definition of target volumes in patients with brain metastases (13).

Based on those recent PET studies, MET-PET images were imported in the planning software for the SRT-IMRT dosimetry as the supplemental information in this preliminary study, and the final target volume was defined and drawn on the stereotactic MR image, taking into account the respective contributions of MET-PET and MRI (Fig. 1). In this report, we describe our preliminary experience with the complementary use of PET metabolic data in an HT system, which uses a patented multileaf collimator to modulate the intensity of the beam, precisely conforming to the shape of the tumor, so it can deliver IMRT technique (14-18). There was no acute or subacute neurologic toxicity from SRT-IMRT in all our cases.

Data from this study demonstrated the utility of MET-PET imaging in monitoring the characteristic changes following SRT-IMRT. By quantitative statistical evaluation, the differences in L/N ratios between the pre-SRT-IMRT group and 3-month post-SRT-IMRT group was significant ($P<.0001$) and that between the pre-SRT-IMRT group and 6-month post-SRT-IMRT group was also significant ($P<.0001$) (Fig. 2). It would seem that those significant decreases of MET uptake could be secondary to metabolic changes

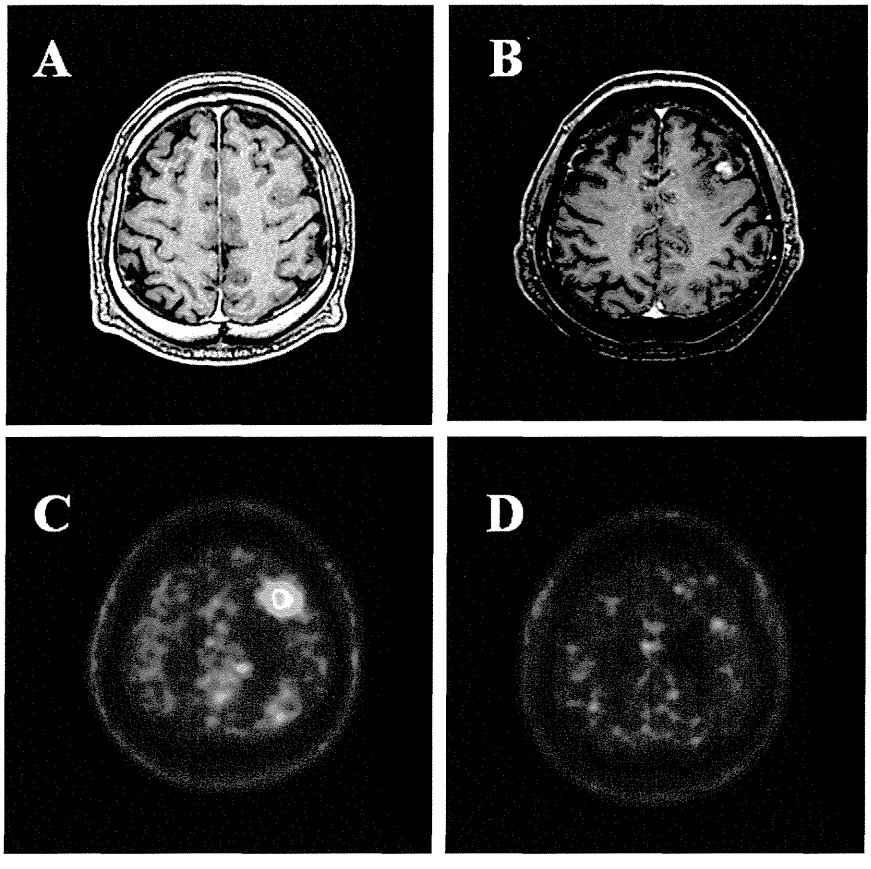

Fig. 4. A 53-year-old male patient with non-small cell lung cancer. Gadolinium-enhanced MRI before SRT-IMRT (A) and 3 months after SRT-IMRT (B), and MET-PET before SRT-IMRT (C) and 3 months after SRT-IMRT (D). Metastatic brain tumor in the left frontal lobe is demonstrated, showing no Gd-enhancement at all on MRI but high MET uptake on PET (A and C). At 3 months after SRT-IMRT, the volume of Gd-enhanced lesion on MRI increased, although MET uptake at the lesion distinctly decreased (B and D). The lesion remained stable in size on MRI after a long-term follow-up, which was assumed to be radiation necrosis.

of target lesion, which suspected the intensive radiosurgical efficacy to the metabolic condition in tumors. The result suggested that reduced MET uptake following SRT-IMRT should be attributed to deactivation and/or obliteration of viable cancer cells after radiation treatment, although other explanations, such as changes in the vasculature or edema/inflammation, must also be considered for the reason of reduced MET uptake. From the follow-up study, marginal tumor recurrence was defined in 2 of 42 tumors, with increasing MET uptake after SRT-IMRT. Local tumor control by SRT-IMRT seemed to be favorable from the results of the follow-up study, so that contouring of the GTV by respective contributions of MET-PET and MRI were thought to be acceptable. Eighteen tumors were lost to follow-up at 6 months after SRT-IMRT. However, we believe that selection bias could be avoided because the reason patients were lost to follow-up was not from neurological death by the metastatic brain tumor.

The present analysis demonstrates that MET-PET containing metabolic information is independent of the morphologic information provided by MRI. The significant difference of MET uptake had been demonstrated in the L/N ratio between the pre-SRT-IMRT group and the post-SRT-IMRT group, irrespective of the type of MRI examination (Fig. 3). In 6 tumors of type C with decreasing MET uptake lesions showed spontaneous shrinkage or remained stable in size on MRI after a long-term follow-up, which was suspicious for radiation injury rather than tumor recurrence (Fig. 4). In the previous report, early delayed reactions occurred from a few weeks to several months later than the subacute reactions following conventional fractionated radiation therapy or radiosurgery (19). This was probably due to temporary demyelination and vascular damage and may prove fully or partially reversible. Tumor swelling sometimes occurs in the early delayed phase and is associated with edema in the surrounding normal brain. Tumor shrinkage occurs later, with subsidence of the surrounding edema. Similarly, contrast enhancement at this time, particularly in the tumor perimeter, reflects a host of reactive responses and not tumor activity. Sometimes it is not easy to distinguish this phenomenon from tumor recurrence with conventional Gd-DTPA-enhanced MR examinations (20).

In the follow-up study after RT, the value of MET-PET was reported to be a sensitive and accurate technique for differentiating between tumor recurrence and radiation injury following stereotactic radiosurgery (9). The current study demonstrates the dynamic change of metabolic condition with MET-PET studies before and after SRT-IMRT, which seems to be appropriate for the differential diagnosis of tumor recurrence from radiation injury. Especially in cases with increasing volume on MRI after SRT-IMRT, results of the dynamic change of MET-PET studies might be helpful for clinical diagnoses. We considered the fact that because MRI has high sensitivity but poor specificity, it should be used first as a screening test. In the event of suspected tumor recurrence, additional MET-PET investigation seems to differentiate between post-treatment changes and tumor recurrence and to avoid both under- and overtreatment, although further studies are needed.

Conclusions

In conclusion, MET-PET seems to have a potential role in providing additional information for treatment by SRT-IMRT, although MRI remains the gold standard for the diagnosis and follow-up of metastatic brain tumors. The present study is a preliminary approach, and the sample size of the study seems to be small for this evaluation, but to more clearly define the impact of PET-based SRT-IMRT planning and monitoring, further experimental and clinical analyses are required.

References

1. Chen W. Clinical applications of PET in brain tumors. *J Nucl Med* 2007;48:1468-1481.
2. Herholz K, Coope D, Jackson A. Metabolic and molecular imaging in neuro-oncology. *Lancet Neurol* 2007;6:711-724.
3. Evans ES, Hahn CA, Kocak Z, et al. The role of functional imaging in the diagnosis and management of late normal tissue injury. *Semin Radiat Oncol* 2007;17:72-80.
4. Levivier M, Massager N, Wikler D, et al. Use of stereotactic PET images in dosimetry planning of radiosurgery for brain tumors: clinical experience and proposed classification. *J Nucl Med* 2004;45: 1146-1154.
5. Grosu AL, Lachner R, Wiedenmann N, et al. Validation of a method for automatic image fusion (BrainLAB System) of computed tomography data and 11C-methionine-PET data for stereotactic radiotherapy using a LINAC: first clinical experience. *Int J Radiat Oncol Biol Phys* 2003;56:1450-1463.
6. Levivier M, Wikler D, Goldman S, et al. Integration of the metabolic data of positron emission tomography in the dosimetry planning of radiosurgery with the gamma knife: early experience with brain tumors. Technical note. *J Neurosurg* 2000;93(suppl):S233-S238.
7. Levivier M, Massager N, Wikler D, et al. Integration of functional imaging in radiosurgery: the example of PET scan. *Prog Neurol Surg* 2007;20:68-81.
8. Jacobs AH, Kracht LW, Gossmann A, et al. Imaging in neurooncology. *NeuroRx* 2005;2:333-347.
9. Tsuyuguchi N, Sunada I, Iwai Y, et al. Methionine positron emission tomography of recurrent metastatic brain tumor and radiation necrosis after stereotactic radiosurgery: is a differential diagnosis possible? *J Neurosurg* 2003;98:1056-1064.
10. Ross DA, Sandler HM, Balter JM, et al. Imaging changes after stereotactic radiosurgery of primary and secondary malignant brain tumors. *J Neurooncol* 2002;56:175-181.
11. Pirotte B, Goldman S, Massager N, et al. Combined use of 18F-fluorodeoxyglucose and 11C-methionine in 45 positron emission tomography-guided stereotactic brain biopsies. *J Neurosurg* 2004;101: 476-483.
12. Baumert BG, Rutten I, Dehing-Oberije C, et al. A pathology-based substrate for target definition in radiosurgery of brain metastases. *Int J Radiat Oncol Biol Phys* 2006;66:187-194.
13. Matsuo M, Miwa K, Shinoda J, et al. Target definition by C11-methionine-PET for the radiotherapy of brain metastases. *Int J Radiat Oncol Biol Phys* 2009;74:714-722.
14. Baisden JM, Benedict SH, Sheng K, et al. Helical TomoTherapy in the treatment of central nervous system metastasis. *Neurosurg Focus* 2007;22:E8.
15. Bauman G, Yartsev S, Fisher B, et al. Simultaneous infield boost with helical tomotherapy for patients with 1-3 brain metastases. *Am J Clin Oncol* 2007;30:38-44.
16. Bauman G, Yartsev S, Rodrigues G, et al. A prospective evaluation of helical tomotherapy. *Int J Radiat Oncol Biol Phys* 2007;68:632-641.
17. Yartsev S, Kron T, Cozzi L, et al. Tomotherapy planning of small brain tumours. *Radiother Oncol* 2005;74:49-52.
18. Welsh JS, Patel RR, Ritter MA, et al. Helical tomotherapy: an innovative technology and approach to radiation therapy. *Technol Cancer Res Treat* 2002;1:311-316.
19. Plowman PN. Stereotactic radiosurgery. VIII. The classification of postradiation reactions. *Br J Neurosurg* 1999;13:256-264.
20. Nishimura R, Takahashi M, Morishita S, et al. MR Gd-DTPA enhancement of radiation brain injury. *Radiat Med* 1992;10:109-116.